Rev.Adv.Mater.Sci. 8 (2004) 97-100

STRUCTURAL AND OPTICAL PROPERTIERS OF β-$FeSi_2$ PHASE PREPARED BY ION BEAM SYNTHESIS

R. Ayache[1], A. Bouabellou[2], F. Eichhorn[3] and E. Richter[3]

[1]Pharmacy Department, University of Batna, 05000, Algeria
[2] Laboratoire des Couches Minces et Interfaces, Université de Constantine, Route de Ain El-Bey, 25000- Algeria
[3]Forschungszentrum Rossendorf, Institut für Ionenstrahlphysik und Materialforschung, Postfach 510119, D-01314 Dresden, Germany

Received: November 9, 2004

Abstract. Semiconducting iron disilicide (β–$FeSi_2$) was prepared by ion beam synthesis (IBS) in (111)Si P-type by implantation at 440 °C of 195 KeV Fe ions with a dose of $2 \cdot 10^{17}$ Fe^+/cm^2 followed by annealing in a N_2 atmosphere at 900 °C for 4 h. Characterization of samples included Rutherford backscattering spectrometry (RBS), X-ray diffraction (XRD) pole figure, and Raman spectroscopy. A mixture of β-$FeSi_2$ and α-$FeSi_2$ was observed in the as-implanted state. A Photoluminescence (PL) measurement at 12K indicates the luminescence peak at the energy of about 0.81 eV corresponding to the band gap energy of β-$FeSi_2$ phase.

1. INTRODUCTION

Ion beam synthesis (IBS) has been widely used for the formation of epitaxial silicides [1,2]. So far most studies focused on transition metal silicides, such as $CoSi_2$ [3] and $FeSi_2$ [4,5]. The iron silicide $FeSi_2$ is of particular interest. It exists in two phases. The tetragonal α–$FeSi_2$ (lattice parameters a=b=0.269 nm and c=0.514 nm) is a metallic phase [6], and the orthorhombic β-$FeSi_2$ is semiconducting phase with lattice parameters a=0.9863 nm, b=0.7791 nm and c=0.7833 nm at room temperature [7]. During the last few years, there has been considerable interest in the fabrication of buried semiconducting iron disilicide (β–$FeSi_2$) layers for a Si-based light emitter with a wavelength (~ 1.5 μm) corresponding to optical fiber communications [8,9], infrared detectors and thermoelectronics devices [10].

In this paper, we report the results of the formation of buried layers of iron disilicide by IBS and the characterizations using RBS, XRD pole figure, Raman spectroscopy and PL.

2. EXPERIMENTAL DETAILS

The (111)Si p-type substrate was implanted with a 195 KeV beam of ^{56}Fe at a current density of 11 μA/cm^2 and a dose of $2 \cdot 10^{17}$ Fe^+/cm^2, the tilt angle of the substrate relative to the beam was 7°. The implantation was carried out at 440 °C. The as-implanted samples were then annealed in N_2 atmosphere at 900 °C for 4h.

Rutherford backscattering measurements were performed on the as-implanted and annealed samples, with 1.7 MeV He^+ ions at a scattering angle of 170° between the incoming and outgoing beam line, and the experimental spectra were analyzed with Rump computer program [11]. XRD pole figure measurements were performed in a θ-2θ geometry using Cu K_a radiation. Raman spectra were measured at room temperature (RT) between 150 and 600 cm^{-1} by dispersive spectrometer combined with a focal microscope. Laser produced light at 532.15 nm was used for excitation. PL measurements were performed at 12K using the 633.4 nm line of the He-

Corresponding author: R. Ayache, e-mail: r_ayache@excite.com

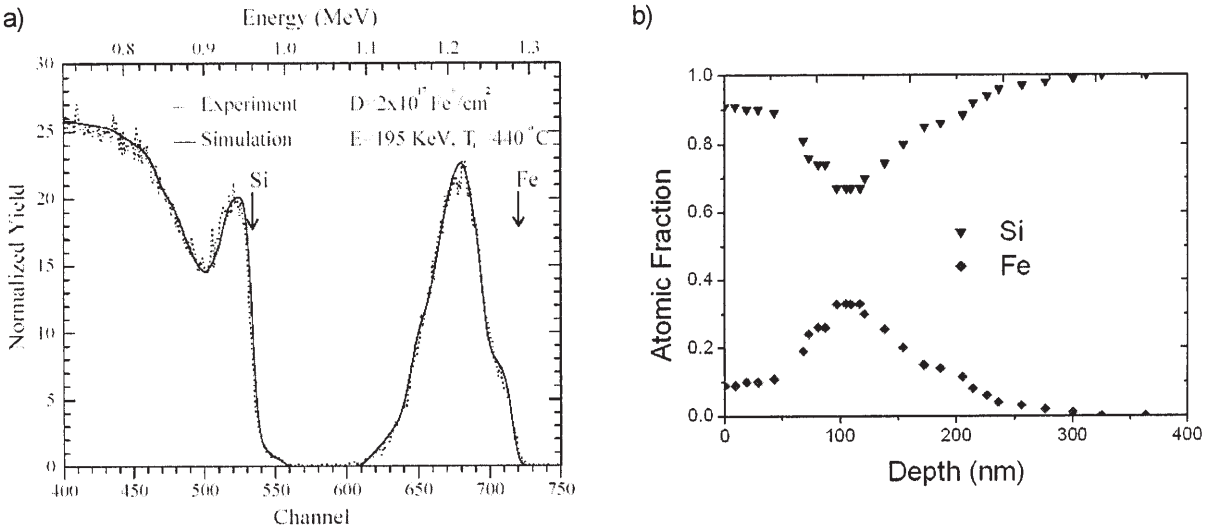

Fig. 1. (a) RBS spectrum for the as-implanted samples; (b) Fe and Si depth profiles deduced from (a).

Ne laser. The emission was detected using a liquid nitrogen-cooled Ge detector.

3. RESULTS AND DISCUSSION

Fig. 1a shows the RBS spectrum of (111)Si sample in the as-implanted state with an ion dose of $2 \cdot 10^{17}$ Fe^+/cm^2 at a substrate temperature of 440 °C, obtained in the random direction. The arrows (labeled Fe and Si) indicate the energy for backscattering from these elements at the surface. The Rump simulation of RBS spectrum allowed to obtain the depth profiles of Si and Fe elements (see Fig. 1b) and to confirm the formation of buried $FeSi_2$ layer during the ion implantation.

Fig. 2 shows the RBS spectra of the as-implanted and annealed samples. As can be seen, the height of Fe signal decreases whereas the energetic width increases. In the same time the Si signal, around channel 500, corresponding to the buried layer is extended to the surface.

Fig. 3a shows the XRD pole figures of the as-implanted sample. The poles are measured with steps of 5° of φ and χ angles (φ is the rotation angle around the surface normal and χ is the tilt angle of the sample) in the whole range of φ and in the range χ=25-50°. The poles with heights of 33.18, 42.70 and 56.97 are produced by the tails of the (111) Si reflections (its maximum is located at 2θ=28.443°) of the substrate. They give the orientation of the substrate. At the scattering angle 2θ=29.112°, the poles with the heights of 5.57, 6.84 and 6.88 which located at 85°/35°, 200°/40° and 315°/35° in the φ/χ coordinates respectively are (220) β-$FeSi_2$/(202) β-$FeSi_2$ reflections. This shows that the β-$FeSi_2$ crystals are oriented in the Si substrate. Furthermore, the intensity peak in the centre of the pole figure indicates β-$FeSi_2$ crystals with a fiber texture. Their epitaxial relationship is described as follows: (220) β-$FeSi_2$ and / or (202) β-$FeSi_2$ || (111)Si. It should be

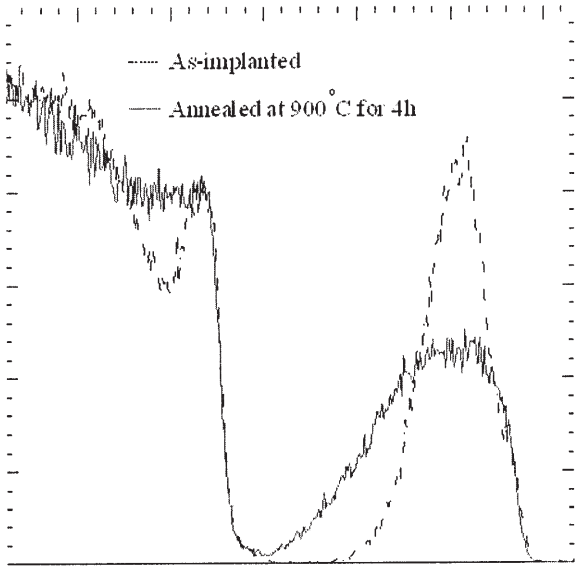

Fig. 2. RBS spectra for the as-implanted and annealed samples.

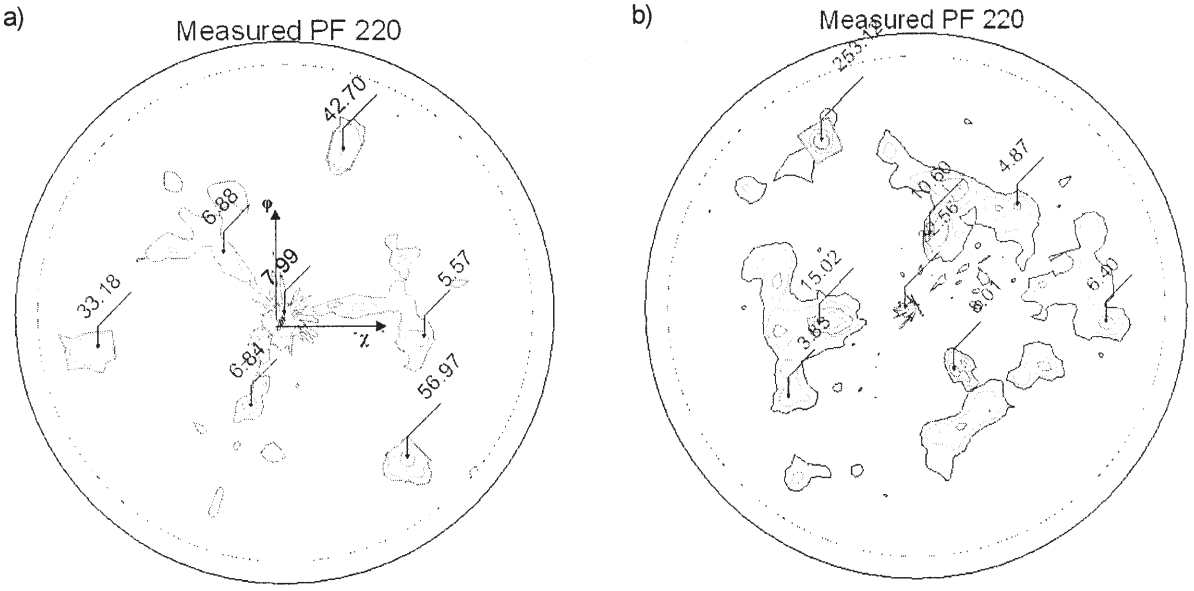

Fig. 3. XRD pole figures for the as-implanted (a) and annealed (b) samples.

noticed that only a very small amount of α-$FeSi_2$ phase was found in this sample.

The XRD pole figures of the annealed sample in N_2 atmosphere at 900 °C for 4h are shown in Fig. 3b. As can be seen, the three poles near the centre and at scattering angle 2θ=29.112° with the heights of 8.01, 15.02 and 10.60 (with j/c: 150°/30°, 260°/40° and 10°/30° respectively) are (220) β-$FeSi_2$ / (202) β-$FeSi_2$ reflections. The other peaks are produced by the tails of (111)Si reflections at 2θ=28.443°.

These results indicate also the formation of epitaxial (220) and / or (202) β-$FeSi_2$ on the (111)Si substrate.

The intensities of three poles of β-$FeSi_2$ are increased in the case of the annealed sample, attesting the increase in amount of β-$FeSi_2$ (width of a buried layer).

Fig. 4 shows the Raman scattering spectra obtained at RT from the as-implanted and annealed samples. The crystalline silicon has a typical line at 520 cm^{-1}. If the silicon becomes amorphous, this line disappears [12,13]. The Raman signals of the annealed sample are clearly identified at 175.8, 194.5, 198.2 and 247.5 cm^{-1}, which are found to originate from Fe-Si vibrational modes [14], reflecting the formation of β-$FeSi_2$ phase. The additional weak peak at 303.5 cm^{-1} is originated from the silicon substrate (the LA phonon). In comparison with the annealed sample, the Raman peaks of the as-implanted sample are located at 186.7, 241.2 and 515.2 cm^{-1}, have smallest intensities and are red-shifted. All experimental signals for β-$FeSi_2$ are slightly shifted toward lower energies compared to those obtained theoretically [14]. This shift may be explained by the stress caused during the implantation and the heat treatment.

PL spectrum obtained at 12K for sample annealed at T_a=900 °C for 4h is shown in Fig. 5. The main feature is an intense peak at 0.81 eV with a line width of approximately 29 meV and we assign this peak to optical radiative transitions intrinsic to β-$FeSi_2$. This light emission, at the wavelength of 1.53 μm, corresponds to the band gap energy of β-$FeSi_2$. The peak of PL measurements performed at low temperature must be come from the β-$FeSi_2$

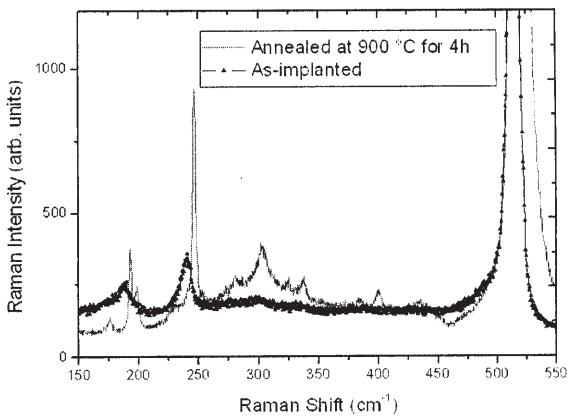

Fig. 4. Raman scattering spectra at RT for the as-implanted and annealed samples.

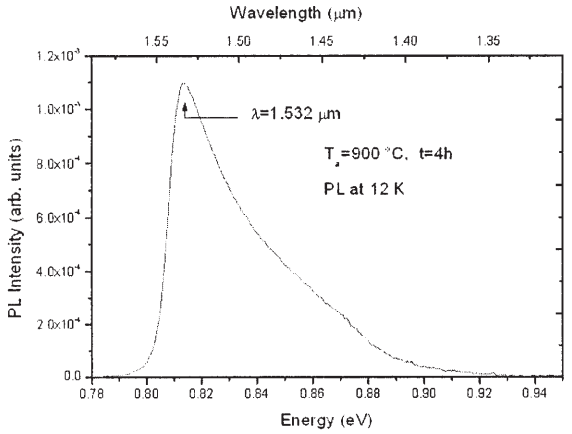

Fig. 5. PL spectrum measured at 12K of β-$FeSi_2$ layer for the annealed sample.

precipitates, as already reported [15]. It is important to notice that the peak position coincides with that of the well known *D1* line emission (0.807 eV) recorded at high temperature [16].

4. CONCLUSION

The β-$FeSi_2$ phase was fabricated by IBS with a dose of $2 \cdot 10^{17}$ Fe^+/cm^2 in (111)Si substrates at 440 °C followed by annealing at 900 °C for 4h. The buried layer is grown epitaxially on (111)Si substrate with the relation of (220) and/or (202) β-$FeSi_2$ || (111)Si. The Raman signals for β-$FeSi_2$ are slightly shifted toward lower energies. In PL measurements, the intense peak was observed at 0.81 eV which is assigned to optical radiative transitions intrinsic to β-$FeSi_2$ silicide. No PL emission was observed for the as-implanted samples.

ACKNOWLEDGEMENTS

With great pleasure, we would like to thank the working team on iron silicide at the Forschungszentrum Rossendorf (Dresden) where much of the experimental work presented here was performed. We will not mention all the names of the people who certainly feel our deepest gratitude. A special thank goes to Dr. R. Grötzschel for the RBS analyses, S. Sinning for his help with the PL measurements and U. Lucchesi for the IR and Raman spectroscopies.

REFERENCES

[1] D.J. Oostra, D.E.W. Vandenhoudt, C.W. T. Bulle-Lieuwma and E. P. Naburgh // *Appl. Phys. Lett.* **59** (1991) 1737.

[2] K. Radermacher, S. Mantl, Ch. Dieker and H. Luth // *Appl. Phys. Lett.* **59** (1991) 2145.

[3] E. H. A. Dekempeneer, J. J. M. Ottenheim, D. W. E. Vandenhoudt, C.W. T. Bulle-Lieuwma and E. G. C. Lathouwers // *Appl. Phys. Lett.* **59** (1991) 467.

[4] D. Gerthsen, K. Radermacher, Ch. Deiker and S. Mantl // *J. Appl. Phys.* **71** (1992) 3788.

[5] N. Kobayashi, H. Katsumata, H. L. Shen, M. Hasegawa, Y. Makita, H. Shibata, S. Kimura, A. Obara , S. Uekusa and T. Hatano // *Thin Solid Films* **270** (1995) 406.

[6] J. Chevrier, P. Stocker, Le Thanh, J. M. Gay and J. Derrien // *Europhys. Lett.* **22** (1993) 449.

[7] Y. Dusaussoy, J. Protas, R. Wandji and B. Roques // *Acta. Cryst. B* **27** (1971) 1209.

[8] D. Leong, M. Harry, J. K. Reeson and K. P. Homewood // *Nature* **387** (1997) 686.

[9] Y. Ozawa, T. Ohtsuka, Cheng Li, T. Suemasu and F. Hasegawa // *J. Appl. Phys.* **95** (2004) 5483.

[10] A. Heinrich, H. Griessmann, G. Behr, K. Ivanko, J. Schumann and Vinzelberg // *Thin Solid Films* **381** (2001) 287.

[11] L. R. Dooltttle // *Nucl. Instr. And Meth. B* **9** (1985) 344.

[12] K. Lefki, P. Muret, E. Bustrarret, N. Boutarek, R. Madar, J. Chevrier, J. Derrien and M. Brunel // *Solid State Communications* **80** (1991) 791.

[13] T. Yoshitake, T. Nagamoto and K. Nagayama // *Thin Solid Films* **381** (2001) 236.

[14] H. Kakemoto, Y. Makita, S. Sakuragi and T. Tsukamoto // *Jpn. J. Appl. Phys.* **38** (1999) 5192.

[15] Y. Gao, S. P. Wong, W. Y. Cheung, G. Shao and K. P. Homewood // *Appl. Phys. Lett.* **83** (2003) 42.

[16] R. Sauer, J. Weber and J. Stolz // *Appl. Phys. A: Mater. Sci. Process.* **36** (1985) 1.